Original
ISSN 2413-0516

Dosimetric and Radiobiological Comparison of IMRT Versus 3DCRT Treatment Plans for Hypofractionated Left-Sided Breast 10 MV Photon Irradiation: A Single Center Study

Hanouf H. Alghanmi[1,2], E.M. Abdelrazek[3], Ehab Attalla[4], Mazen Al Gaoud[5], Nasser Al Dhaibani[5], Hosam Mohamed Ibrahim Salaheldin[1*]

[1]Biophysics Research Group, Physics Department, Faculty of Science, Mansoura University, Mansoura, Egypt.
[2]Department of Radiation Oncology, King Abdulaziz Medical City, Ministry of National Guard Health Affairs, Jeddah, 21423, Saudi Arabia.
[3]Physics Department, Faculty of Science, Mansoura University, Mansoura, Egypt.
[4]National Cancer Institute, Cairo University, Giza, Egypt.
[5]Department of Radiation Oncology, King Abdullah Medical City, Jeddah, Saudi Arabia.
*Correspondence to: Hosam Mohamed Ibrahim Salaheldin (E-mail: hsmohamed@mans.edu.eg)
(Submitted: 29 May 2025 – Revised version received: 05 July 2025 – Accepted: 01 August 2025 – Published online: 26 October 2025)

Abstract

Objective: This study aims to perform a dosimetric and radiobiological comparison between Three-Dimensional Conformal Radiotherapy (3DCRT) and Intensity-Modulated Radiotherapy (IMRT) for a hypofractionated regimen.

Methods: A retrospective analysis was conducted on fifty patients with left-sided, node-negative breast cancer after breast-conserving surgery. Treatment plans were generated for each patient using both 3DCRT (field-in-field technique) and IMRT (inverse-planned with 5 fields) techniques for a prescription dose of 40.05 Gy in 15 fractions. Plans were evaluated based on dosimetric parameters for planning target volume (PTV) coverage (Dmin, Dmean, V95%, V105%), conformity (CI), homogeneity (HI), and doses to OARs (heart, lungs, spinal cord). Radiobiological evaluation included calculating Tumor Control Probability (TCP) and Normal Tissue Complication Probability (NTCP).

Results: IMRT demonstrated significantly superior PTV coverage, with higher Dmin (27.55 vs. 16.54 Gy, $P < 0.0001$), V95% (99.81% vs. 87.55%, $P < 0.0001$), and ideal conformity (CI = 1.00 vs. 0.87, $P < 0.0001$). However, IMRT resulted in a larger volume receiving 105% of the dose (V105% = 44.68% vs. 11.70%, $P < 0.0001$). For OARs, IMRT reduced the mean heart dose (3.40 vs. 2.51 Gy, $P < 0.0001$) and ipsilateral lung V20Gy (17.42% vs. 18.21%, $P = 0.31$), but increased low-dose exposure (e.g., heart V10Gy and lung V5Gy). IMRT demonstrated a superior TCP (96.2% compared to 93.1%, $P < 0.0001$) and IMRT demonstrated a superior TCP (96.2% compared to 93.1%, $P < 0.0001$) and markedly reduced NTCP for radiation pneumonitis (2.1% versus 19.2%, $P < 0.0001$) and cardiac problems (0.10% versus 0.20%, $P < 0.0001$). NTCP for radiation pneumonitis (2.1% versus 19.2%, $P < 0.0001$) and cardiac problems (0.10% versus 0.20%, $P < 0.0001$). IMRT required substantially more monitor units and longer beam-on time.

Conclusion: IMRT offers a dosimetrically and radiobiologically enhanced plan for hypofractionated radiation treatment of left-sided breast cancer, ensuring superior target coverage and a marked decrease in the anticipated risk of pulmonary and cardiac problems. Nonetheless, this strategy incurs the expense of heightened low-dose exposure to adjacent tissues and increased complexity in treatment administration. The selected approach must be tailored according to patient anatomy and specific risk profiles.

Keywords: Breast cancer, radiotherapy, 3DCRT, IMRT, dosimetric comparison, NTCP, TCP, hypofractionation

Introduction

Breast cancer is the most common life-threatening malignancy in women and the leading cause of cancer-related mortality worldwide, accounting for 15.3% of all diagnoses and 7% of deaths. In early-stage disease, adjuvant breast-conserving surgery with whole-breast radiotherapy reduces regional recurrence and improves survival.[1,2] Three-dimensional conformal radiotherapy (3DCRT) and intensity-modulated radiotherapy (IMRT) are widely used for breast cancer treatment to optimize target coverage while sparing organs at risk. Compared with conventional 2D tangential beams, 3DCRT employs gantry angles, field-in-field (FIF) techniques, dose weighting, multi-leaf collimator (MLC) shaping, and beam energy selection to improve breast coverage and reduce heart and lung exposure. The MLC further limits cardiac and pulmonary volumes within the radiation field. Forward-planned IMRT uses tangential beams with additional manually conformed FIF segments to enhance dose homogeneity, thereby eliminating the need for wedges, which otherwise increase monitor units and scatter dose to healthy tissues.[3–5]

IMRT, an advanced form of 3DCRT, modulates beam intensity to enhance treatment precision and dose conformity. In left-sided breast cancer, the concave chest wall inevitably exposes portions of the heart and lung to radiation. IMRT mitigates this by improving dose homogeneity and sparing normal tissues through greater planning flexibility. Widely demonstrated to outperform 3DCRT in sites such as the head and neck, central nervous system, lung, and prostate, IMRT employs MLCs to modulate fluence and deliver the prescribed dose to the target while minimizing exposure to organs at risk. For breast cancer, particular concern lies in the heart and lungs, especially given the cardiotoxicity of systemic agents such as anthracyclines, taxanes, and trastuzumab.[6–9]

Inverse intensity-modulated radiotherapy uses predefined beam arrangements, target coverage objectives, and organ-at-risk (OAR) constraints to generate optimized intensity-modulated plans. This approach provides superior dose conformity and OAR sparing by tailoring radiation delivery to the tumor's geometry. However, IMRT increases the integral dose to surrounding healthy tissues, raising concerns about secondary malignancies in long-term survivors.[10]

Comparing 3DCRT and IMRT is essential for optimizing treatment in post-mastectomy left-sided breast cancer. Our department employs a hypofractionated regimen of 40.05 Gy in 15 fractions (2.67 Gy per fraction) based on the United Kingdom Standardization of Breast Radiotherapy Trial B protocol trial, which demonstrated equivalent efficacy and reduced toxicity compared with conventional 50 Gy in 25 fractions. Consistent with Jones et al., we incorporate radiobiological modeling into clinical decision-making, using biologically effective dose calculations referenced to 60 Gy in 30 fractions to validate hypofractionated schedules.[11]

The aim of this study is to compare 3DCRT and IMRT in post-mastectomy left-sided breast cancer treated with a hypofractionated regimen of 40.05 Gy in 15 fractions under deep inspiration breath-hold (DIBH) using uniform 10 MV photon beams. This represents the first single-center analysis from the Middle Eastern region in this context. The study integrates dosimetric evaluation with equivalent uniform dose (EUD)-based Tumor Control Probability (TCP) and Normal Tissue Complication Probability (NTCP) modeling for cardiac and pulmonary risks, alongside practical deliverability parameters such as monitor units and beam-on time, providing region-specific, clinically relevant insights into the safety, efficacy, and practicality of modern hypofractionated breast radiotherapy.

Materials and Methods

Patient Selection

A retrospective cohort of 50 women with early-stage (Stage I–II) left-sided breast cancer who underwent breast-conserving surgery and had histologically negative axillary lymph nodes was analyzed. Eligible patients were aged 25–70 years. Patients with prior thoracic radiotherapy, bilateral breast malignancy, or major comorbidities affecting respiratory function were excluded.

CT Simulation and Immobilization

All patients underwent CT simulation in the supine position using a Q-fix breast board (Avondale, PA, USA). For larger breast volumes, the board was elevated to 15° to reduce overlap between the breast and humeral head. Arms were elevated using hand support sticks, and two indexers secured the board to the treatment couch to ensure reproducible lateral and longitudinal positioning. Simulation was performed under DIBH using the Real-Time Position Management system (Varian Medical Systems, Palo Alto, CA, USA). A four-dot reflective marker block placed on the xiphoid process monitored respiratory motion, with a gating window of 4 mm to maintain breath-hold reproducibility. CT images were acquired on a GE simulator and reconstructed at 4-mm slice intervals.

Targets and OARs Delineations

CT images were acquired from the C3 vertebra to 5 cm inferior to the inframammary fold. The datasets were imported into the Eclipse treatment planning system (version 18.0, Varian Medical Systems, Palo Alto, CA, USA) for target and OAR delineation as well as dose calculation. Contouring of targets and OARs, including the heart, lungs, and spinal cord, was performed on the DIBH scans in accordance with the Radiation Therapy Oncology Group (RTOG) breast cancer atlas guidelines.[12] The PTV was generated by expanding the clinical target volume with a 5 mm margin, and an additional 2 mm skin flash was applied to ensure adequate superficial coverage.

Planning Techniques and Beam Configuration

All treatment plans prescribed 40 Gy in 15 fractions to the PTV, with OARs constraints based on RTOG recommendations. Treatments were delivered on a Varian TrueBeam linear accelerator equipped with kilovoltage imaging and a MLC, consisting of 80 central leaves with 0.5 cm resolution and 40 peripheral leaves with 1 cm resolution at isocenter. Dose calculations were performed in Eclipse v18.0 using the Acuros XB algorithm with dose-to-medium reporting, a 2.5 mm grid, and heterogeneity correction. Each case was replanned using 3DCRT and IMRT to assess the impact of beam geometry and modulation on dosimetric and radiobiological outcomes. Optimization goals included PTV coverage of D90% ≥ 90%, mean heart dose ≤ 4 Gy, ipsilateral lung V20 Gy ≤ 30%, and a maximum spinal cord dose < 10 Gy.

3DCRT (Field-in-Field/Tangential Fields)

Two opposing tangential fields were employed at gantry angles designed to minimize overlap with the lung and heart (typically 305°–315° for the medial field and 135°–125° for the lateral field). A FIF technique was incorporated to improve dose homogeneity and ensure adequate PTV coverage by supplementing underdosed regions within the prescription isodose line. Beam energies of 10 MV were selected for patients presenting with larger separations. Tangential fields were planned using a half-beam block technique, with jaws closed at the central axis to limit beam divergence into the ipsilateral lung and heart.

IMRT (Five Non-Coplanar Fields)

For IMRT planning, inverse IMRT with 10 MV photon beams was employed to optimize target coverage and OAR sparing. Unlike forward-planned IMRT or field-in-field tangential techniques, which rely on manual selection of beam weights and segments, inverse IMRT uses computer-based optimization to automatically determine the optimal beamlet intensities needed to meet predefined dosimetric objectives. This approach allows greater flexibility in shaping dose distributions, particularly in complex geometries such as left-sided breast cancer, where cardiac and pulmonary sparing is critical. Beam arrangements consisted of 5 coplanar fields with individualized gantry angles designed to encompass the whole breast volume while minimizing entry through the contralateral breast, lung, and heart. Beam geometry was tailored to patient anatomy, considering chest wall curvature and breast separation, in order to enhance dose conformity and reduce hotspots within the PTV.

Intensity modulation was achieved using a dynamic multileaf collimator technique, in which the MLC leaves move continuously while dose rate is adjusted dynamically during beam delivery. This enabled generation of highly conformal dose distributions and improved homogeneity inside the PTV compared to 3DCRT and forward-planned IMRT. Collimator rotations of 5°–10° were introduced to limit interleaf transmission, and jaw settings were adjusted to restrict beam divergence into the ipsilateral lung and heart. Inverse optimization was performed in Eclipse v17.0 using the Acuros XB

algorithm (dose-to-medium, 2.5 mm grid size, heterogeneity correction enabled). Planning objectives were standardized across all patients, including PTV coverage of D90% ≥ 90%, mean heart dose ≤ 4 Gy, ipsilateral lung V20 Gy ≤ 30%, and maximum spinal cord dose < 10 Gy. Iterative adjustment of objective weightings was used during optimization to achieve a balance between target coverage and OAR sparing while avoiding over-modulation and excessive MU usage.

Evaluation Parameters

Dosimetric and radiobiological analyses were performed to comprehensively evaluate the quality of each treatment plan and to predict potential clinical outcomes. Dosimetric assessment included evaluation of target coverage, dose homogeneity, and conformity, as well as quantification of dose received by OARs. Radiobiological analysis involved calculation of parameters such as TCP and NTCP to estimate the clinical impact of the delivered dose distributions.

Target Coverage Metrics

Dosimetric evaluation of the PTV included the following parameters: Dmin (Gy), the minimum point dose within the PTV; Dmax (Gy), the maximum point dose; Dmean (Gy), the mean dose; D2% (Gy), representing the near-maximum dose received by 2% of the PTV. Volumetric coverage metrics included V90% (%), the volume of the PTV receiving at least 90% of the prescription dose; V95% (%), the volume receiving at least 95%; and V105% (%), the volume receiving more than 105% of the prescription dose.

OAR Metrics

For OARs, heart dosimetry included the mean dose, D5% representing the near-maximum dose received by 5% of the heart volume, and V10%, the volume receiving ≥10% of the prescription dose. Ipsilateral lung parameters included V5%, V10%, and V20%, indicating the volumes receiving ≥5%, ≥10%, and ≥20% of the prescription dose, while the contralateral lung was evaluated using V5 Gy as a low-dose spread indicator. Spinal cord exposure was quantified using Dmax, defined as the maximum point dose delivered to 0.1 cm^3 of the structure. Radiobiological assessment involved calculation of TCP and NTCP to estimate the clinical implications of the delivered dose distributions.

Dose Gradient and Spill Measures

Plan quality was further evaluated using the Conformity Index (CI) and Homogeneity Index (HI). The CI was defined as the ratio of the volume receiving 100% of the prescription dose to the PTV volume, providing a measure of dose conformity. The HI was calculated as (D2%–D98%)/D50%, assessing dose uniformity within the PTV and indicating the degree of dose homogeneity across the target volume.

Delivery Metrics

Treatment delivery parameters were also evaluated, including the total number of MUs per plan, as recorded by the treatment planning system, and beam-on time, calculated by dividing the total MUs by the average dose rate and cross-validated with the recorded treatment console logs.

Calculating the NTCP and TCP Using a Biological Model

The equivalent uniform dose (EUD) model was used for calculating the TCP.

$$NTCP = \frac{1}{1+\left(\frac{TD50}{EUD}\right)^{4\gamma 50}} \quad (1)$$

The TCD50 is the dose for controlling 50 percent of the tumors when the tumor is homogeneously irradiated. γ50 is the slope of the dose response curve. The Lyman-EUD model combines EUD with the LKB NTCP model:

$$NTCP = \frac{1}{1+\left(\frac{TD50}{EUD}\right)^{4\gamma 50}} \quad (2)$$

Where TD50 is the tolerance dose for a 50% complication rate at a specific time interval. Also, EUD can be calculated from Eq.(3) as follows:

$$EUD = \left(\sum v_i D_i^a\right)^{1/a} \quad (3)$$

Where (*vi*) is the organ volume that receives a dose (*Di*) while (*a*) is a tissue-specific parameter describing the volume effect. IIn this work, the (*a*) value as well as other parameters TCD50 and γ50 were taken as listed in Table 1. For comparative aim, the values for TCD50 and γ50 for adjuvant radiotherapy and curative aim were studied in order to evaluate the TCP values with physical obtain from DVH.[13] The radiobiological parameters (a, γ50, TD50) listed in Table 1 were selected based on their widespread adoption and validation in prior foundational literature for modeling breast radiotherapy outcomes. These equations were written in MATLAP in order to analyze the DVH for each patient using the specific program.

Table 1. **Radiobiological parameters used to calculate NTCP and TCP**

Structures		a	γ50	TCD_{50}	TD_{50}	α/β	References
Tumor	Breast	–7.2	2	28		4	Willner et al.[15] Guerreo et al.[13] Hall et al.[14]
OARs	Heart	3	3		48	3	
	lung	3	2		24.5	3	Emami et al.[16]
	Spinal cord	7.4	4		66.5	3	

The MATLAB funtion used was eudmodel.m (EUDMODEL), where DVH is a two-column matrix representing the cumulative, rather than the differential, dose–volume histogram. The first column corresponds to increasing absolute dose or percentage dose values, and the second column corresponds to the corresponding absolute or relative volume values. The matrix must have a minimum of two rows and both columns must be of equal length.

Statistical Evaluation

Statistical analysis was performed using IBM SPSS Statistics version 20.0 (IBM Corp, Armonk, NY, USA). The calculation results were expressed as the mean value and standard deviation. The results were compared using a two-sample paired *t*-test. A *P*-value of less than 0.05 ($P < 0.05$) was considered statistically significant with a 95% confidence interval.

Results

A dosimetric and radiobiological comparison was performed for 50 left-sided breast cancer patients replanned with 3DCRT and IMRT for a hypofractionated regimen of 40.05 Gy in 15 fractions. The analysis highlighted a key trade-off: IMRT achieved superior target coverage and reduced high-dose OAR exposure, but at the expense of greater low-dose spread and higher treatment complexity.

IMRT demonstrated clear superiority in target coverage, as shown in Table 2. The V95% was significantly higher with IMRT (99.81 ± 0.18% vs. 87.55 ± 7.61%, $P < 0.0001$), and the minimum dose to the PTV (Dmin) was markedly improved (27.55 ± 9.76 Gy vs. 16.54 ± 10.11 Gy, $P < 0.0001$), indicating better coverage of peripheral regions often underdosed with 3DCRT. IMRT also achieved ideal conformity (CI = 1.00 ± 0.00 vs. 0.87 ± 0.08, $P < 0.0001$) and superior homogeneity (HI = 0.06 ± 0.03 vs. 0.20 ± 0.19, $P < 0.0001$). These advantages, however, were accompanied by a substantially larger hotspot volume (V105%: 44.68 ± 16.34% vs. 11.70 ± 6.49%, $P < 0.0001$), reflecting the dose heterogeneity characteristic of IMRT optimization.

The OAR analysis revealed a nuanced pattern central to the technique selection dilemma, as shown in Table 2. For the heart, IMRT produced a characteristic low-dose bath, with a significantly greater V10Gy (35.24 ± 10.97% vs. 4.93 ± 3.68%, $P < 0.0001$) and lower mean dose (2.51 ± 1.24 Gy vs. 3.40 ± 0.54 Gy, $P < 0.0001$). A similar trend was observed for the ipsilateral lung, where IMRT substantially increased low-dose exposure (V5Gy: 74.30 ± 12.18% vs. 29.80 ± 6.07%; V10Gy: 41.80 ± 9.41% vs. 22.35 ± 5.23%, $P < 0.0001$ for both). Importantly, no significant difference was observed in V20Gy (17.42 ± 5.53% vs. 18.21 ± 4.64%, $P = 0.31$), the key predictor of radiation pneumonitis.

For other OARs, IMRT modestly reduced contralateral lung exposure (V5Gy: 6.21 ± 4.67% vs. 8.49 ± 6.31%, $P = 0.005$), while the maximum spinal cord dose was higher but remained well below established tolerance limits. The dosimetric advantages of IMRT were accompanied by a marked increase in treatment complexity. IMRT plans required approximately 6.5-fold more monitor units (2066 ± 515 vs. 314 ± 30, $P < 0.0001$), which translated into a 77% longer beam-on time per fraction (2.19 ± 0.36 min vs. 1.23 ± 0.05 min, $P < 0.0001$).

Table 2. **Comparison of dosimetric and treatment delivery parameters for the PTV and OARs between 3DCRT and IMRT. Data are presented as mean ± standard deviation ($N = 50$)**

	Parameters	Mean ± SD		*P*-value
		3DCRT (A)	IMRT (B)	(A) vs (B)
PTV	D_{min} (Gy)	16.54 ± 10.11	27.55 ± 9.76	<0.0001
	D_{max} (Gy)	43.35 ± 0.52	45.41 ± 0.68	<0.0001
	D_{mean} (Gy)	39.60 ± 1.43	41.87 ± 0.36	<0.0001
	$D_{2\%}$ (Gy)	42.65 ± 1.57	43.75 ± 0.37	<0.0001
	$V_{90\%}$ (%)	97.36 ± 4.33	99.99 ± 0.05	<0.0001
	$V_{95\%}$ (%)	87.55 ± 7.61	99.81 ± 0.18	<0.0001
	$V_{105\%}$ (%)	11.70 ± 6.49	44.68 ± 16.34	<0.0001
	CI	0.87 ± 0.08	1.00 ± 0.00	<0.0001
	HI	0.20 ± 0.19	0.06 ± 0.03	<0.0001
Heart	D_{Mean} (Gy)	3.40 ± 0.54	2.51 ± 1.24	<0.0001
	$D_{5\%}$ (Gy)	13.62 ± 12.10	18.84 ± 1.87	0.002
	V_{10Gy} (%)	4.93 ± 3.68	35.24 ± 10.97	<0.0001
Lt. Lung	V_{5Gy} (%)	29.80 ± 6.07	74.30 ± 12.18	<0.0001
	V_{10Gy} (%)	22.35 ± 5.23	41.80 ± 9.41	<0.0001
	V_{20Gy} (%)	18.21 ± 4.64	17.42 ± 5.53	0.31
Rt. Lung	V_{5Gy} (%)	8.49 ± 6.31	6.21 ± 4.67	0.005
Spinal. cord	D_{Max} (Gy)	0.42 ± 0.16	7.50 ± 1.09	0.002
Total no of MUs	MU	314 ± 30	2066 ± 515	<0.0001
Beam-on time	Treatment time (Min)	1.23 ± 0.05	2.19 ± 0.36	<0.0001

The comparative analysis demonstrated a clear dosimetric advantage of IMRT over 3DCRT. As shown in Figure 1, IMRT achieved superior dose conformity to the PTV, reducing high-dose spillage into surrounding healthy breast tissue, while 3DCRT showed heterogeneous dose distribution. The DVH analysis (Figure 2) confirmed IMRT provided more homogeneous PTV dose coverage and significantly reduced ipsilateral lung V20Gy and mean heart dose, indicating lower radiation-induced morbidity risk compared to 3DCRT.

Radiobiological modeling helped clarify the paradox of increased low-dose exposure with IMRT, as shown in Table 3. For the PTV, IMRT achieved a significantly higher equivalent uniform dose (EUD: 42.0 ± 0.9 Gy vs. 38.5 ± 4.91 Gy, $P < 0.0001$), corresponding to a 3.1% absolute gain in predicted tumor control probability (TCP: 96.2% vs. 93.1%, $P < 0.0001$).

For normal tissues, despite greater low-dose exposure, IMRT's superior sparing of high-dose regions resulted in lower predicted normal tissue complication probabilities (NTCP), particularly for the heart (0.10% vs. 0.20%, $P < 0.0001$) and ipsilateral lung. The latter demonstrated the most pronounced benefit, with the predicted risk of radiation pneumonitis reduced nearly tenfold (2.1% vs. 19.2%, $P < 0.0001$). A sensitivity analysis, varying the model parameters within published confidence intervals, confirmed that the statistically significant superiority of IMRT in reducing NTCP for pneumonitis and heart complications remained robust.

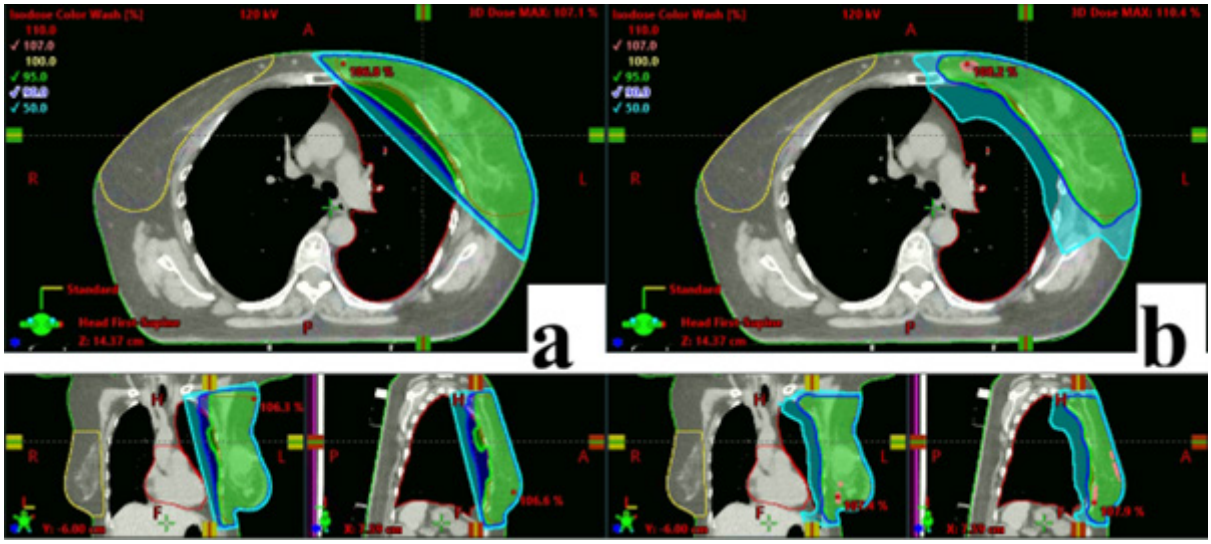

Fig. 1 **Dose distribution comparison. (A) 3DCRT and (B) IMRT plans shown in axial, sagittal, and coronal views. IMRT demonstrates improved target conformity and reduced high-dose exposure to organs at risk.**

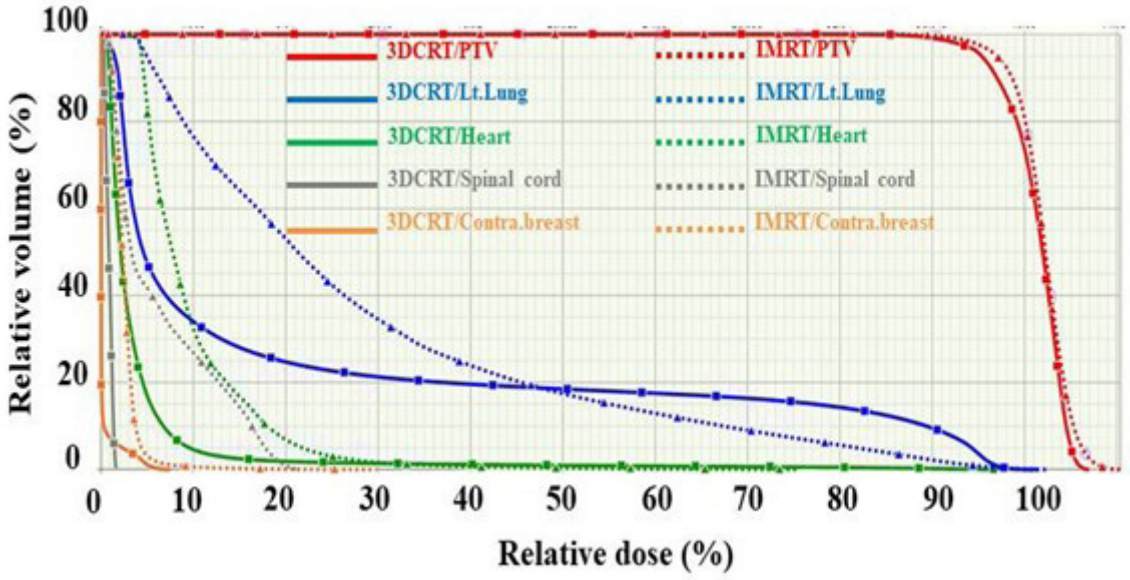

Fig. 2 **DVH comparison for 3DCRT and IMRT plans using a 10 MV beam. The IMRT plan (solid lines) yields a steeper, more homogeneous dose gradient across the PTV compared to the 3DCRT plan (dashed lines).**

Table 3. **Comparison of radiobiological parameters (EUD, NTCP, and TCP) between 3DCRT and IMRT for the PTV and OARs**

	Parameters	Mean ± SD		*P*-value
		3DCRT (A)	IMRT (B)	(A) vs (B)
PTV	EUD (Gy)	38.5 ± 4.91	42.0 ± 0.9	<0.0001
	TCP (%)	93.1 ± 2.47	96.2 ± 0.6	<0.0001
Heart	EUD (Gy)	8.1 ± 3.63	6.8 ± 1.3	0.014
	NTCP (%)	0.20 ± 0.15	0.10 ± 0.08	<0.0001
Lt. Lung	EUD (Gy)	20.3 ± 4.0	14.2 ± 1.8	<0.0001
	NTCP (%)	19.2 ± 20.55	2.1 ± 2.5	<0.0001
Rt. Lung	EUD (Gy)	0.13 ± 0.06	1.70 ± 0.45	<0.0001
	NTCP (%)	0.0 ± 0.0	0.0 ± 0.0	N/A
Spinal. cord	EUD (Gy)	0.15 ± 0.07	3.01 ± 0.80	<0.0001
	NTCP (%)	0.0 ± 0.0	0.0 ± 0.0	N/A

Discussion

This study compares the dosimetric, delivery and radiobiological outcomes of 3DCRT and IMRT in hypofractionated treatment of left-sided, node-negative breast cancer after breast-conserving surgery. IMRT provided superior target coverage and OAR sparing but resulted in higher low-dose exposure and greater treatment complexity compared with 3DCRT. These findings underscore the need for patient-specific selection of radiotherapy techniques based on anatomical and clinical risk factors.

In 3DCRT, beam angles and weights are manually selected based on diagnostic imaging to generate a conformal dose distribution around the target volume. MLCs are used to shape the beams according to the tumor's projection. By contrast, IMRT employs inverse planning, in which the desired dose distribution and OAR constraints are defined first, and computer algorithms subsequently determine the optimal beam intensities. IMRT utilizes dynamic MLCs to modulate beam intensity, enabling complex dose distributions with concave isodose lines around critical structures. Typically, IMRT incorporates five to nine fields compared with the two fields commonly used in 3DCRT, facilitating improved dose conformity. However, IMRT planning necessitates advanced optimization algorithms and more rigorous quality assurance procedures.[17]

IMRT significantly improved target coverage relative to 3DCRT, yielding higher Dmin, Dmean, V90%, and V95% values for the PTV. The CI reached ideal values (1.00 ± 0.00) with IMRT, indicating highly precise dose distributions. These results are consistent with previous studies reporting the superiority of IMRT in breast cancer radiotherapy. However, improved coverage was accompanied by an increase in the V105%, reflecting the characteristic dose heterogeneity of IMRT. Overall, IMRT demonstrates enhanced conformity and homogeneity while sparing normal tissues, with the capacity to generate concave dose distributions particularly advantageous in left-sided breast cancers and other anatomically complex sites such as head and neck cancers.[18] IMRT yielded mixed dosimetric outcomes, reducing the mean heart dose and ipsilateral lung V20Gy but increasing low-dose exposure to the heart and lung at V10Gy and V5Gy, reflecting the characteristic low-dose bath of multi-field techniques. The principal advantage of IMRT lies in its ability to reduce high-dose exposure to organs at risk while preserving adequate target coverage.[19]

Our radiobiological analysis predicted a markedly reduced risk of radiation pneumonitis with IMRT compared with 3DCRT (NTCP: 2.1% vs. 19.2%), representing a clear clinical advantage for patients with pulmonary compromise or those receiving concurrent therapies. IMRT also demonstrated a lower NTCP for cardiac complications (0.10% vs. 0.20%) despite increased low-dose volumes. These findings are consistent with a multicenter analysis showing that IMRT reduces acute toxicity in adjuvant whole-breast radiotherapy and with meta-analytic evidence confirming reduced rates of grade 2 pneumonitis. The reduced NTCP despite increased low-dose exposure may be explained by the disproportionate contribution of high-dose regions to complications in serial organs. IMRT's ability to limit high-dose exposure outweighs the impact of increased low-dose regions, a particularly important factor in left-sided breast cancer.[20,21]

While the absolute reduction in mean heart dose with IMRT was modest (2.51 vs. 3.40 Gy), its clinical relevance is supported by the linear no-threshold model of radiation-associated cardiac risk, in which any dose reduction is considered potentially beneficial for long-term survivors. Conversely, the large reduction in pneumonitis NTCP (19.2% to 2.1%) is likely to translate into a highly meaningful clinical benefit. Our model also predicted a higher TCP with IMRT compared with 3DCRT (96.2% vs. 93.1%). Overall, these results align with existing evidence demonstrating improved cardiac sparing and superior OAR constraint fulfillment with advanced techniques. Nevertheless, IMRT delivers a higher integral dose to normal tissues due to increased low-dose exposure from multiple beam angles. Importantly, the NRG Oncology–RTOG 0617 trial reported comparable secondary cancer rates between IMRT and 3DCRT (6.6% vs. 5.5%). The conformal dose distributions achievable with IMRT may also enable safe dose escalation without increasing toxicity.[22]

A key distinction between 3DCRT and IMRT lies in treatment delivery time. Longer IMRT sessions increase the risk of intrafraction motion and reduce departmental throughput. IMRT also requires substantially higher MUs, resulting in greater integral body dose from head leakage and scattered radiation. In this study, IMRT plans required 6.5 times more MUs and twice the beam-on time compared with 3DCRT, impacting workflow and patient comfort. While 3DCRT remains advantageous for patients with straightforward anatomy due to its simplicity and efficiency, IMRT may be justified in cases with complex anatomy or higher risk of complications. VMAT can achieve similar dosimetric benefits to IMRT with reduced delivery time, and hybrid approaches combining 3DCRT with limited IMRT may offer a balance between plan quality and efficiency. However, IMRT demands greater planning time and rigorous quality assurance, including pretreatment verification, which reduces clinical availability and increases implementation costs. Institutional resources and expertise must therefore be considered when selecting between these techniques.[23]

Conclusion

Incorporating dosimetric evaluation, EUD-based TCP/NTCP modeling, and treatment delivery parameters, this study

showed that IMRT provides superior target coverage and reduced cardiac and pulmonary exposure compared with 3DCRT, albeit at the cost of increased low-dose exposure and greater delivery complexity. These findings highlight the need to individualize technique selection based on patient anatomy, toxicity risk, and institutional resources, with IMRT favored for complex or high-risk cases and 3DCRT remaining suitable for simpler scenarios.

Conflict of Interest

None.

References

1. Youlden, D., Cramb, S., Yip, C., & Baade, P. (2014). Incidence and mortality of female breast cancer in the Asia-Pacific region. Cancer Biology & Medicine, 11(2):101–115. https://doi.org/10.7497/j.issn.2095-3941.2014.02.005
2. Cl arke, M., Collins, R., Darby, S., Davies, C., Elphinstone, P., Evans, V., Godwin, J., Gray, R., Hicks, C., James, S., Mackinnon, E., McGale, P., McHugh, T., Peto, R., Taylor, C., & Wang, Y. (2005). Effects of radiotherapy and of differences in the extent of surgery for early breast cancer on local recurrence and 15-year survival: an overview of the randomised trials. The Lancet, 366(9503):2087–106. https://doi.org/10.1016/S0140-6736(05)67887-7
3. Phansopkar, D., Sachdeva, J., Mahajan, M., Kingsley, P., Upadhyay, S., & Chakravarti, R. (2015). Tangential beam intensity modulated radiotherapy versus tangential beam three-dimensional conformal radiotherapy in carcinoma breast: A dosimetric comparison and clinical correlation. Korean Journal of Clinical Oncology, 11(2):120-125. https://doi.org/10.14216/KJCO.15020.
4. Haciislamoglu, E., Çolak, F., Canyılmaz, E., Dirican, B., Gurdalli, S., Yilmaz, A., Yoney, A., & Bahat, Z. (2015). Dosimetric comparison of left-sided whole-breast irradiation with 3DCRT, forward-planned IMRT, inverse-planned IMRT, helical tomotherapy, and volumetric arc therapy. Physica Medica, 31(4):360–367. https://doi.org/10.1016/j.ejmp.2015.02.005.
5. Liu, T., Sun, T., Chen, J., & Zhang, G. (2015). SU-E-T-17: A Comparison of Forward and Field in Field Intensity Modulation Radiotherapy Planning for Breast Cancer. Medical Physics, 42(6):3334. https://doi.org/10.1118/1.4924378.
6. Rastogi, K., Sharma, S., Gupta, S., Agarwal, N., Bhaskar, S., & Jain, S. (2018). Dosimetric comparison of IMRT versus 3DCRT for post-mastectomy chest wall irradiation. Radiation Oncology Journal, 36(1): 71–78. https://doi.org/10.3857/roj.2017.00381.
7. Fisher, B., Jeong, J., Anderson, S., Bryant, J., Fisher, E., & Wolmark, N. (2002). Twenty-five-year follow-up of a randomized trial comparing radical mastectomy, total mastectomy, and total mastectomy followed by irradiation. The New England Journal of Medicine, 347(8):567–75. https://doi.org/10.1056/NEJMOA020128.
8. Veronesi, U., Cascinelli, N., Mariani, L., Greco, M., Saccozzi, R., Luini, A., Aguilar, M., & Marubini, E. (2002). Twenty-year follow-up of a randomized study comparing breast-conserving surgery with radical mastectomy for early breast cancer. The New England Journal of Medicine, 347(16):1227–32. https://doi.org/10.1056/NEJMOA020989.
9. Lohr, F., El-Haddad, M., Dobler, B., Grau, R., Wertz, H., Kraus-Tiefenbacher, U., Steil, V., Madyan, Y., & Wenz, F. (2009). Potential effect of robust and simple IMRT approach for left-sided breast cancer on cardiac mortality. International Journal of Radiation Oncology, Biology, Physics, 74(1):73–80. https://doi.org/10.1016/j.ijrobp.2008.07.018.
10. Narayanasamy, G., Granatowicz, D., Baacke, D., Li, Y., Gutierrez, A., Papanikolaou, N., & Stathakis, S. (2015). A Comparison between Three-Dimensional Conformal Radiotherapy, Intensity-Modulated Radiotherapy, and Volumetric-Modulated Arc Therapy Techniques for Stereotactic Body Radiotherapy of Lung Tumors. International Journal of Medical Physics, Clinical Engineering and Radiation Oncology, 4(2):104–112. https://doi.org/10.4236/IJMPCERO.2015.42014.
11. Jones, B., Dale, R., Deehan, C., Hopkins, K., & Morgan, D. (2001). The role of biologically effective dose (BED) in clinical oncology. Clinical Oncology (Royal College of Radiologists (Great Britain)), 13(2):71–81. https://doi.org/10.1053/CLON.2001.9221.
12. Thibault F, Benamor M, Tardivon A. Breast cancer: Atlas. Rev Prat. 2004 Apr 30;54(8):837–8, 840.
13. Guerrero, M., & Li, X. (2003). Analysis of a large number of clinical studies for breast cancer radiotherapy: estimation of radiobiological parameters for treatment planning. Physics in Medicine & Biology, 48:3307–3326. https://doi.org/10.1088/0031-9155/48/20/004.
14. Hall EJ (2000): Radiobiology for the radiologist. 5th ed. LippincoQ Williams & Wilkins. USA.
15. Jochen Wi, Kurt Ba r, Ekaterini Ca, Axel Ts and Michael Fl (2002): Dose, volume, and tumor control predictions in primary radiotherapy of non-small-cell lung cancer. Int J Radiat Oncol Biol Phys; 52(2):382–89. Doi: 10.1016/s0360-3016(01)01823-5.
16. Emami B, Lyman J, BrownA, Coia L, Goitein M, Munzenrider JE, Shank B, Solin LJ and Wesson M (1991): Tolerance of normal tissue to therapeutic irradiation. Int J Radiat Oncol Biol Phys, 21(1):109–122. Doi: 10.1016/0360-3016(91)90171-y.
17. Bakiu, E., Telhaj, E., Kozma, E., Ruçi, F., & Malkaj, P. (2013). Comparison of 3D CRT and IMRT Tratment Plans. Acta Informatica Medica, 21(3):211–212. https://doi.org/10.5455/aim.2013.21.211-212.
18. Jagsi, R., Griffith, K. A., Moran, J. M., Matuszak, M. M., Marsh, R., Grubb, M., ... & Michigan Radiation Oncology Quality Consortium. (2022). Comparative effectiveness analysis of 3D-conformal radiation therapy versus intensity modulated radiation therapy (IMRT) in a prospective multicenter cohort of patients with breast cancer. International Journal of Radiation Oncology* Biology* Physics, 112(3):643–653. https://doi.org/10.1016/j.ijrobp.2021.09.053.
19. Sá, A. C., Barateiro, A., Bednarz, B. P., Almeida, P., Vaz, P., & Madaleno, T. (2022). Comparison of 3DCRT and IMRT out-of-field doses in pediatric patients using Monte Carlo simulations with treatment planning system calculations and measurements. Frontiers in Oncology, 12, 879167. https://doi.org/10.3389/fonc.2022.879167
20. Hu, X., He, W., Wen, S., Feng, X., Fu, X., Liu, Y., & Pu, K. (2016). Is IMRT Superior or Inferior to 3DCRT in Radiotherapy for NSCLC? A Meta-Analysis. PLoS ONE, 11. https://doi.org/10.1371/journal.pone.0151988.
21. Chen, S., Ramachandran, P., & Deb, P. (2020). Dosimetric comparative study of 3DCRT, IMRT, VMAT, Ecomp, and Hybrid techniques for breast radiation therapy. Radiation Oncology Journal, 38:270–281. https://doi.org/10.3857/roj.2020.00619.
22. Chun, S., Hu, C., Komaki, R., Timmerman, R., Schild, S., Bogart, J., Dobelbower, M., Bosch, W., Kavadi, V., Narayan, S., Iyengar, P., Robinson, C., Rothman, J., Raben, A., Augspurger, M., MacRae, R., Paulus, R., & Bradley, J. (2024). Long-Term Prospective Outcomes of Intensity Modulated Radiotherapy for Locally Advanced Lung Cancer: A Secondary Analysis of a Randomized Clinical Trial. JAMA Oncology. 10(8):1111–1115. https://doi.org/10.1001/jamaoncol.2024.1841.
23. Duan, L., Qi, W., Chen, Y., Cao, L., Chen, J., Zhang, Y., & Xu, C. (2023). Evaluation of complexity and deliverability of IMRT treatment plans for breast cancer. Scientific Reports, 13:21474. https://doi.org/10.1038/s41598-023-48331-x.